Meshless boundary element methods for exterior problems on spheroids

E.P.Stephan[1], A.Costea[1] ,Q.T.Le Gia[2] and T. Tran[2]

[1] Institute for Applied Mathematics and QUEST (Center for Quantum Engineering and Space-Time Research), Leibniz University of Hanover, Am Welfengarten 1, 30167 Hanover, Germany.
E-mail: Stephan@ifam.uni-hannover.de

[2] School of Mathematics and Statistics, University of New South Wales, Sydney, NSW 2052, Australia. Email: qlegia@unsw.edu.au, Thanh.Tran@unsw.edu.au,

Keywords: Boundary integral equations, meshless methods, preconditioning, domain decomposition

Abstract. In geophysical applications one is interested in the Neumann problem exterior to a spheroid where the orbits of satellites are located. The satellites create data which amount to boundary conditions in scattered points. As a model problem, we consider the exterior Neumann problem of the Laplacian with boundary condition on an oblate or prolate spheroid. We propose to use spherical radial basis functions in the solution of the boundary integral equation arising from the Dirichlet-to-Neumann map. Our meshless approach with radial basis functions is particularly suitable for handling scattered satellite data. We also propose a preconditioning technique based on an overlapping domain decomposition method to deal with ill-conditioned matrices arising from the approximation problem.

Here we report from [14, 11] on a meshless method with radial basis functions for the Neumann problem for the Laplacian exterior to an oblate or a prolate spheroid. In geophysical applications [1, 2] one is interested in such exterior Neumann problems where the orbits of satellites are located on spheroids. A key tool of our approach is the use of the Dirichlet-to-Neumann map which directly converts the bounday value problem into a pseudodifferential equation on the spheroid. This integral equation is then handled with Fourier techniques by expansion into appropriate spherical harmonics. Huang and Yu [6] solved this pseudodifferential equation numerically with standard boundary elements on a regular grid on the angular domain of the spherical coordinates. Our approach uses spherical radial basis functions (SRBF's) instead, allowing for better handling of scattered data. Originally we introduced the meshless boundary element method for integral equations on the sphere [4] and we used it to solve the linearized Molodensky problem [3]. The error analysis for the meshless method with radial basis functions on the sphere as done in [4] has been extended to spheroids in [14, 11]. Again the smooth solution of the pseudodifferential equation can be approximated with high convergence rates by the Galerkin solution consisting of radial basis functions. The numerical solution is obtained by an appropiate implementation [9] of the prolate and oblate spheroidal harmonics and by truncating the resulting infinite dimensional discrete Galerkin system.

We present numerical results of our meshless boundary element method for equidistributed points, so-called Saff points, and for scattered data points from satellite observations. Furthermore we present iteration numbers for the conjugate gradient method applied to solve the discrete systems in case of scattered data. We list the iteration numbers for the preconditioned conjugate gradient method when an overlapping additive Schwarz method is used as preconditioner. For both oblate and prolate spheroids we obtain only mildly growing iteration numbers for the overlapping additive Schwarz method. This technique was firstly analysed for pseudodifferential equations on the sphere in [5].

Let $\Gamma_0 = \{(x_1, x_2, x_3): \frac{x_1^2}{a^2} + \frac{x_2^2}{a^2} + \frac{x_3^2}{b^2} = 1, a > b > 0\}$ be an oblate spheroid and Ω^c be the unbounded domain outside the boundary Γ_0.

We consider the exterior Neumann problem: Given $g \in L_2(\Gamma_0)$, find $U \in \Omega^c$ satisfying

$$\begin{aligned} &\Delta U = 0 && in \quad \Omega^c \\ &\partial_\nu U = g && on \quad \Gamma_0 \\ &U(\mathbf{x}) = O(||\mathbf{x}||^{-1}) && as \quad ||\mathbf{x}|| \to \infty \end{aligned} \tag{1}$$

where $||\mathbf{x}||$ denotes the Euclidean norm of $\mathbf{x}$ and ν denotes the unit outward normal vector on Γ_0.

The solution is given by the series

$$U(\mu,\theta,\varphi) = \sum_{n=0}^{\infty} \sum_{m=-n}^{n} \frac{T_n^m(\sinh\mu)}{T_n^m(\sinh\mu_0)} \hat{u}_{nm} Y_{nm}(\theta,\varphi), \quad \mu \geq \mu_0 > 0,$$

where (μ,θ,φ) denote the oblate spheroidal coordinates [6]. Here

$$T_n^m = i\exp(\frac{i\pi n}{2})Q_n^m(ix), \quad i^2 = -1,$$

and Q_n^m are the associated Legendre functions of second kind and Y_{nm} the spherical harmonics of degree n and $\hat{u}_{nm}$ the expansion coefficients.

In [6] it is shown that eq (1) is equivalent to

$$\mathcal{K}u = g \quad on \quad \Gamma_0 \tag{2}$$

with the Dirichlet-to-Neumann map (Steklov-Poincaré operator) $\mathcal{K}$. Its weak formulation is: Find $u \in H^{1/2}(\Gamma_0)$ satisfying

$$D(u,v) := \int_{\Gamma_0} (\mathcal{K}u)v\,ds = \int_{\Gamma_0} gv\,ds \quad \forall v \in H^{1/2}(\Gamma_0) \tag{3}$$

$$with \quad D(u,v) = f_0 \sum_{n=0}^{\infty} \sum_{m=-n}^{n} G_n^m(\sinh\mu_0)\hat{u}_{nm}\hat{v}_{nm}^* \tag{4}$$

$$where \quad G_n^m(x) := -\frac{(1+x^2)\frac{d}{dx}T_n^m(x)}{T_n^m(x)}. \tag{5}$$

Proposition: *There exists a unique solution for the variational problem (3).*

This is due to the Lax-Milgram theorem since $D(\cdot,\cdot)$ is continuous and coercive on the Sobolev space $H^{1/2}(\Gamma_0)$ and the right hand side in eq (3) defines a continuous linear functional on $H^{1/2}(\Gamma_0)$. Here $u \in H^s(\Gamma_0)$, $s \in \mathbb{R}$ if and only if

$$\| u \|_{H^s(\Gamma_0)}^2 = \sum_{n=0}^{\infty} \sum_{m=-n}^{n} (1+n^2)^s |\hat{u}_{nm}|^2 < \infty$$

The approximate solution to eq (3) is sought in a finite dimensional subspace of $H^{1/2}(\Gamma_0)$. In order to use SRBFs we take the bijection $\omega: \Gamma_0 \to \mathbb{S}^2$

$$\omega(\mathbf{x}) = (\sin\theta\cos\varphi, \sin\theta\sin\varphi, \cos\theta), \tag{6}$$

and we define a reproducing kernel on Γ_0 as

$$\Psi(\mathbf{x},\mathbf{x}') = \Phi(\omega(\mathbf{x}),\omega(\mathbf{x}')), \quad \mathbf{x},\mathbf{x}' \in \Gamma_0 \tag{7}$$

where Φ is defined via a univariate function $\phi: [-1,1] \to \mathbb{R}$ by (see [7, 8])

$$\Phi(\mathbf{y},\mathbf{z}) = \phi(\mathbf{y}\cdot\mathbf{z}) \quad \forall\, \mathbf{y},\mathbf{z} \in \mathbb{S}^2. \tag{8}$$

Here ϕ has a series expansion in terms of Legendre polynomials P_n of degree n, as

$$\phi(t) = \frac{1}{4\pi}\sum_{n=0}^{\infty} (2n+1)\hat{\phi}(n)P_n(t) \tag{9}$$

with

$$\hat{\phi}(n) = 2\pi\int_{-1}^{+1} \phi(t)P_n(t)dt. \tag{10}$$

The kernel Ψ can be expanded into a series of spherical harmonics as

$$\Psi(\mathbf{x},\mathbf{x}') = \sum_{n=0}^{\infty} \sum_{m=-n}^{n} \hat{\phi}(n)Y_{nm}(\omega(\mathbf{x}))Y_{nm}^*(\omega(\mathbf{x}')) \tag{11}$$

where we choose

$$\hat{\phi}(n) \cong (1+n^2)^{-\tau}. \tag{12}$$

Given a set of scattered data points $X = \{\mathbf{x}_1, \ldots, \mathbf{x}_M\} \subset \Gamma_0$, we take

$$V^\tau := \ span\,\{\Psi_j := \Psi(\mathbf{x}_j, \cdot) : \mathbf{x}_j \in X\}.$$

Now, the solution of eq (3) is approximated by $u_X \in V^\tau$ satisfying the Galerkin method

$$D(u_X, v) = \int_{\Gamma_0} gv\, ds \quad \forall v \in V^\tau. \tag{13}$$

To this end we have to solve a linear system

$$A\mathbf{c} = \mathbf{g} \tag{14}$$

where A is a matrix with entries $A_{i,j} = D(\Psi_i, \Psi_j), \quad i,j = 1, \ldots, M$ and $\mathbf{g}$ is a vector with entries

$$g_j = \int_{\Gamma_0} g\Psi_j\, ds, \quad j = 1, .., M.$$

Using eq (4) and eq (11) we can write

$$A_{i,j} = f_0 \sum_{n=0}^{\infty} \sum_{m=-n}^{n} [\hat{\phi}(n)]^2 G_n^m(\sinh\mu_0) Y_{nm}(\omega(\mathbf{x}_i)) Y_{nm}^*(\omega(\mathbf{x}_j)). \tag{15}$$

Further let N denote the number of the series terms of the truncated matrix element $A_{i,j}^N$. Then we compute the actual Galerkin approximation u_X by solving eq (14) with the Galerkin matrix A^N obtained via the truncated entries $A_{i,j}^N$.

Let $Y = \mathbf{y}_1, \ldots, \mathbf{y}_M$ be the image of X under the map ω, i.e. $\mathbf{y}_j = \omega(\mathbf{x}_j)$ for $j = 1, \ldots, M$. As Y is a set of scattered points on $\mathbb{S}^2$, we define the mesh norm h_Y of Y as usual $h_Y = \sup_{\mathbf{y} \in \mathbb{S}^2} \min_{\mathbf{y}_j \in Y} \cos^{-1}(\mathbf{y} \cdot \mathbf{y}_j)$.

Proposition [11]: *For an oblate spheroid and truncation number N chosen sufficiently large there holds the quasioptimal error estimate for the difference between the exact solution $u \in H^s(\Gamma_0)$ of eq (3) and the Galerkin solution $u_X \in V^\tau, 2\tau \geq s$*

$$\| u - u_X \|_{H^{1/2}(\Gamma_0)} \leq C h_Y^{s-1/2},$$

where the constant C is independent from N and the set X used to define Ψ_j.
(The corresponding result for the prolate spheroid see [14].)

Our numerical experiments plotted in Fig. 2 for the equidistant mesh of Saff points (see Fig. 1) show these predicted convergence rates α, namely $\alpha = 2.5$ for $Om = 0$ ($\tau = 1.5$), $\alpha = 4.5$ for $Om = 1$ ($\tau = 2.5$), $\alpha = 6.5$ for $Om = 2$ ($\tau = 3.5$), cf. Table 1.

To compute the entries A_{ij} of the stiffness matrix given in eq (15), we need to compute the spherical harmonics Y_{nm} and the functions G_n^m. The functions T_n^m are calculated using the algorithm for oblate spheroidal harmonics presented in (see [9]) and we use $G_n^m(x) = G_n^{-m}(x)$

$$G_n^m(x) = (n+1)x + (n-m+1)\frac{T_{n+1}^m(x)}{T_n^m(x)}, m = 0,1, \ldots, n;\ n = 0,1,2, \ldots$$

The right hand side terms g_j are computed by using the Fourrier coefficients of g and Ψ_j and Parseval's identity.

In our numerical experiments, we use $\Psi(\mathbf{x}, \mathbf{x}') = \Phi(\omega(\mathbf{x}), \omega(\mathbf{x}'))$ for arbitrary $\mathbf{y}, \mathbf{z} \in \mathbb{S}^2$ and $\Phi(\mathbf{y}, \mathbf{z}) = \rho_m(\sqrt{2 - 2\mathbf{y} \cdot \mathbf{z}})$ with ρ_m being locally supported radial basis functions defined by Wendland [10]; see Table 1. In this case eq (12) holds for $\tau = m + 3/2$ see[12].

m	$\rho_m(r)$	τ
0	$(1-r)_+^2$	1.5
1	$(1-r)_+^4(4r+1)$	2.5
2	$(1-r)_+^6(35r^2+18r+3)$	3.5

Table 1: Wendland's RBFs

Example 1: Problem (1) with **oblate spheroid** Γ_0 ($f_0 = 4$, $\mu_0 = 1$), Neumann condition and exact solution

$$g = -\frac{\sinh\mu\sin\theta\cos\varphi\,(2\cosh^2\mu+\cos^2\theta)}{f_0^2(\cosh^2\mu-\cos^2\theta)^{\frac{5}{2}}}$$

$$U = \frac{\cosh\mu\sin\theta\cos\varphi}{f_0^2(\cosh^2\mu-\cos^2\theta)^{\frac{3}{2}}} \tag{16}$$

Let $e := u - u_X$ where $u(\theta,\varphi) = U(\mu_0,\theta,\varphi)$, solves eq (3) and u_X solves eq (13) with truncation number $N_{trunc} = 100$. We compute $\| e \|_{L^2(\Gamma_0)}$ and $\| e \|_{H^{1/2}(\Gamma_0)}$ approximately by $N_{max} = 120$

$$\| e \|_{L^2(\Gamma_0)} \approx \left(\sum_{n=0}^{N_{max}} \sum_{m=-n}^{n} |\widehat{u_X}_{nm} - \hat{u}_{nm}|^2\right)^{1/2}$$

and $$\| e \|_{H^{1/2}(\Gamma_0)} \approx \left(\sum_{n=0}^{N_{max}} (1+n^2)^{1/2} \sum_{m=-n}^{n} |\widehat{u_X}_{nm} - \hat{u}_{nm}|^2\right)^{1/2}$$

$$with \quad \widehat{u_X}_{nm} = \sum_{i=1}^{M} \hat{\phi}(n) c_i Y_{nm}(\omega(\mathbf{x}_i))$$

and $\hat{u}_{nm}$ is computed by an appropriate quadrature formula [13].

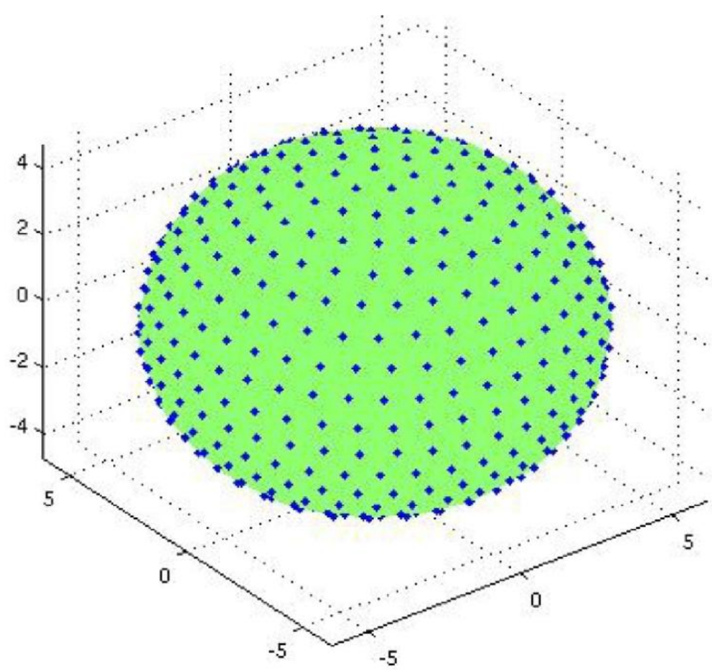

Figure 1: Image of Saff points on oblate spheroid

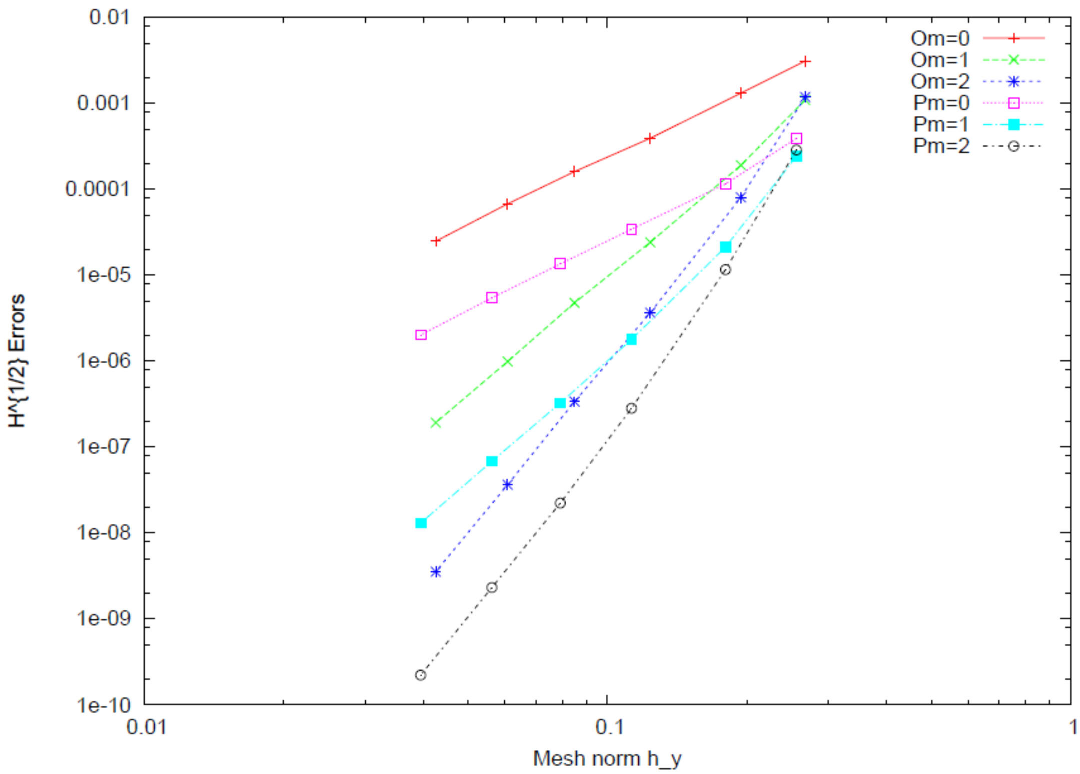

Figure 2: Log-log plot for $H^{1/2}(\Gamma_0)$ errors using Wendland RBFs $\rho_m(r)$ (Saff points) for the oblate (Om) and prolate spheroid (Pm)

Table 2 gives the errors in the $L^2(\Gamma_0)$ and $H^{1/2}(\Gamma_0)$ norms for scattered points. The matrix is ill conditioned and a preconditioner is required. Table 3 shows the corresponding numbers of iteration of the preconditioned conjugate gradient method (PCG) with an overlapping additive Schwarz preconditioner [mref]; stopping criteria in both cases is relative tolerance $\leq 10^{-10}$. Errors of the same order as in the non-preconditioned case are obtained but PCG needs much smaller iteration numbers.(cpu: computational times in seconds, iter: numbers of iterations)

M	q_Y	$\| e \|_{L^2(\Gamma_0)}$	$\| e \|_{H^{1/2}(\Gamma_0)}$	ITER	CPU
3470	$\pi/140$	6.25503E-006	5.01114E-005	2809	234.6
7763	$\pi/200$	2.41695E-006	2.13257E-005	27064	13323.7
10443	$\pi/240$	1.87142E-006	1.62031E-005	30931	17361.9

Table 2: Errors with scattered points from MAGSAT, using CG, $\rho_0(r)$, Ex.1

M	$\cos\alpha$	$\cos\beta$	$\| e \|_{L^2(\Gamma_0)}$	$\| e \|_{H^{1/2}(\Gamma_0)}$	ITER	CPU
3470	0.9	-0.15500000	6.24283E-006	5.02580E-005	73	4.3
7763	0.97	0.99999996	2.41695E-006	2.13257E-005	939	294.1
10443	0.98	0.99999996	1.87142E-006	1.62031E-005	1602	1085.8

Table 3: Errors with scattered points from MAGSAT, for PCG, $\rho_0(r)$, Ex.1

In [14] we have analysed the foregoing meshless boundary element method for a prolate spheroid. We obtain similar results both with respect to convergence of the meshless Galerkin solution as well as the behaviour of the iteration number of PCG. For brevity we present only some numerical results.

Example 2: Problem (1) with **prolate spheroid** Γ_0 ([14]), Neumann condition and exact solution

$$g(\mu,\theta,\varphi) = -\frac{\sqrt{2}\sin 2\theta\cos\varphi\,(7-3\cosh 4\mu+4\cosh 2\mu\cos 2\theta)}{4f_0^4\sqrt{\cosh^2\mu-\cos^2\theta}\,(\cosh 2\mu+\cos 2\theta)^{7/2}}$$

$$U(\mu,\theta,\varphi) = \frac{\sqrt{2}\sinh 2\mu\sin 2\theta\cos\varphi}{2f_0^3(\cosh 2\mu+\cos 2\theta)^{5/2}}. \tag{17}$$

stopping criteria in both cases is relative tolerance $\leq 10^{-10}$.

Tables 4 and 5 give the errors in the $L^2(\Gamma_0)$ and $H^{1/2}(\Gamma_0)$ norms and the iteration numbers for CG and PCG for scattered points for Example 2 (stopping criteria in both cases is relative tolerance $\leq 10^{-8}$). We observe for the prolate spheroid that the errors of the meshless boundary element method and the performance of the PCG with overlapping Schwarz preconditioner behave as in the case of the oblate spheroid.

m	M	q_Y	$\Vert e \Vert_{L^2(\Gamma_0)}$	$\Vert e \Vert_{H^{1/2}(\Gamma_0)}$	cpu	iter
0	2133	$\pi/100$	1.08971E-6	7.79793E-6	19.2	1124
	7763	$\pi/200$	2.15172E-7	1.81600E-6	1592.3	7518
1	2133	$\pi/100$	3.76100E-8	2.54359E-7	102	7737
	7763	$\pi/200$	1.03461E-8	6.99365E-8	620.6	4059

Table 4: Errors with scattered points from MAGSAT, using CG, $\rho_m(r)$, Ex.2

m	M	cosα	cosβ	J	cpu	iter	$\Vert e \Vert_{L^2(\Gamma_0)}$
0	2133	0.90	-0.01	42	4.4	68	0.11045E-5
	2133	0.80	-0.66	22	4.6	45	0.11045E-5
	2133	0.70	-0.78	17	5.6	36	0.11045E-5
	2133	0.60	-0.69	11	4.1	22	0.11045E-5
	7763	0.97	0.63	140	176.1	226	0.24240E-6
	7763	0.90	-0.46	48	133.6	85	0.24247E-6
	7763	0.80	-0.76	23	162.1	59	0.24239E-6
	7763	0.70	-0.84	17	238.2	51	0.24239E-6
1	2133	0.90	-0.01	42	10.9	251	0.36969E-7
	2133	0.80	-0.66	22	6.1	95	0.36969E-7
	2133	0.70	-0.78	17	7.9	75	0.36969E-7
	2133	0.60	-0.69	11	2.8	22	0.36969E-7
	7763	0.97	0.63	140	323.3	738	0.36654E-8
	7763	0.90	-0.46	48	104.5	147	0.42327E-8
	7763	0.80	-0.76	23	55.8	40	0.47790E-8
	7763	0.70	-0.84	17	154.8	60	0.35058E-8

Table 5: Errors with scattered points from MAGSAT, for PCG, $\rho_m(r)$, Ex.2

References

[1] Freeden, W. and Gervens, T. and Schreiner, M. *Constructive approximation on the sphere* of Numerical Mathematics and Scientific Computation. The Clarendon Press Oxford University Press, New York, 1998. With applications to geomathematics.

[2] E. W. Grafarend, F. W. Krumm and V.S. Schwarze. *Geodesy: the Challenge of the 3rd Millennium*. Springer, Berlin, 2003.

[3] Stephan, E.P. and Tran, T. and Costea, A. A boundary integral equation on the sphere for high-precision geodesy. *Computer Methods in Mechanics: Lectures of the CMM 2009*, :99--110, 2010.

[4] Tran, T. and Le Gia, Q. T. and Sloan, I. H. and Stephan, E. P. Boundary integral equations on the sphere with radial basis functions: error analysis. *Appl. Numer. Math.*, 59(11):2857--2871, 2009.

[5] Tran, T. and Le Gia, Q. T. and Sloan, I. H. and Stephan, E. P. Preconditioners for pseudodifferential equations on the sphere with radial basis functions. *Technical report, School of Mathematics and Statistics, The University of New South Wales.*, 2009, submitted.

[6] Huang, Hongying and Yu, Dehao. The ellipsoid artificial boundary method for three-dimensional unbounded domains. *J. Comput. Math.*, 27(2-3):196--214, 2009.

[7] Schoenberg, I. J. Positive definite functions on spheres. *Duke Math. J.*, 9:96--108, 1942.

[8] Xu, Yuan and Cheney, E. W. Strictly positive definite functions on spheres. *Proc. Amer. Math. Soc.*, 116(4):977--981, 1992.

[9] Gil, A. and Segura, J. A code to evaluate prolate and oblate spheroidal harmonics. *Computer Physics Communications.*, 108:267--278, 1998.

[10] Wendland, Holger. *Scattered data approximation*, volume 17 of Cambridge Monographs on Applied and Computational Mathematics. Cambridge University Press, Cambridge, 2005.

[11] Costea, A. and Le Gia, Q. T. and Tran, T. and Stephan, E. P. Solution to the Neumann problem exterior to an oblate spheroid by radial basis functions. To appear, 2010.

[12] Narcowich, Francis J. and Ward, Joseph D. Scattered data interpolation on spheres: error estimates and locally supported basis functions. *SIAM J. Math. Anal.*, 33(6):1393--1410 (electronic), 2002.

[13] Driscoll, James R. and Healy, Jr., Dennis M. Computing Fourier transforms and convolutions on the 2-sphere. *Adv. in Appl. Math.*, 15(2):202--250, 1994.

[14] Le Gia, Q. T. and Tran, T. and Stephan, E. P. Solution to the Neumann problem exterior to a prolate spheroid by radial basis functions. *Advances in Computational Mathematics*, 2010.